

Central European Journal of Chemistry

An ab initio simulation of the UV/Visible spectra of substituted chalcones

Research Article

Yunsheng Xue^{a*}, Jie Mou^a, Yi Liu^a, Xuedong Gong^b, Yihua Yang^a, Lin An^a

^a Chemical and Biological Pharmaceutical Engineering Research Center, School of Pharmacy, Xuzhou Medical College, Xuzhou, Jiangsu 221004, China

^b Department of Chemistry, Nanjing University of Science and Technology, Nanjing 210094, China

Received 12 January 2010; Accepted 07 April 2010

Abstract: The electronic absorption spectra of 29 phenyl-ring substituted chalcones have been investigated with the time-dependent density functional theory (TD-DFT) and polarizable continuum TD-DFT (PCM-TD-DFT). It turns out that the hybrid PBE1PBE functional with the 6-31G basis set provide reliable λ_{max} when the solvent effects are included in the model. Comparisons with experimental values lead to a mean absolute error of 12 nm (0.136 eV). Moreover, the observed substituent effects are reproduced by calculation qualitatively. The λ_{max} of substituted chalcone in phenyl ring A is less sensitive to substitution than that in ring B. The linear correlation of Hammett's substituent constants (σ_p) with LUMO energies is better with respect to HOMO energies. The calculation reveals that the maximum absorption band mainly results from the $\pi \rightarrow \pi^*$ transition from HOMO to LUMO. The analysis of the electron density plots of frontier molecular orbitals show that most transitions should be of valence excitation nature.

Keywords: Chalcones • TD-DFT • PCM • Absorption spectrum • Substituent effect

© Versita Sp. z o.o.

1. Introduction

Chalcones are 1,3-diaryl-2-propen-1-ones obtained from both synthetic and natural sources (see Fig. 1). They have a wide variety of biological activities such as ulcer, cancer, HIV, and malaria prevention, acts as a fungicide and antioxidant, and is both anti-inflammatory and anti-mitotic [1-8]. Beyond these very important applications in biological chemistry, chalcones have interesting optical properties including high extinction coefficients for absorption in the UV, and significant nonlinear optical responses [9-15], thus they can be regarded as promising candidates for new nonlinear optical (NLO) materials. Therefore, it is clear that understanding the nature of the main electronic transitions responsible for the absorption spectrum of chalcones is a problem of some practical interest, and a systematic theoretical investigation on absorption spectra of chalcone derivatives is helpful in the exploration of new nonlinear optical materials from chalcone.

Nowadays, quantum chemical calculations have been proven to be an important tool for investigation of the relationship between structures and spectral properties of the organic molecules and for the interpretation of experimental data arising from industrial interest and applications. We are aware of a few theoretical studies of the absorption spectra of chalcones, but they were limited to the semi-empirical PPP and ZINDO approachs [16-21], and did not account for solvation effects. On the other hand, using *ab initio* CIS/HF, Oumi *et al.* [22] studied chalcone and its hydroxyl derivatives, but the differences reported between gas-phase theoretical and solvated experimental λ_{max} are quite large (0.7eV on average). In recent years, time-dependent density functional theory (TD-DFT) has emerged as a reliable standard tool for the theoretical treatment of electronic excitation spectra and recent works demonstrate the good accuracy for a wide range of systems [23-34].

Figure 1. The molecular structure and atomic numbering of trans-

Moreover, the computational cost of TD-DFT calculation is comparative to that of a Hartree–Fock based single excitation theory, such as, configuration interaction singles (CIS) or time-dependent Hartree–Fock (TDHF) method. In addition, bulk solvent effects can be accounted for when using TD-DFT.

In recently published methodological paper [35], we have shown that PCM-TD-PBE1PBE /6-31G// PBE1PBE/6-31G(d) method are successful for reproducing the molecular geometry and absorption wavelength of chalcone. Besides [35], to the best of our knowledge, only three papers have reported on the use of DFT for the study of chalcones. The electron affinities and antioxidant properties of different substituted chalcones have been successfully reproduced by Hicks et al. [36] and Kozlowski et al. [37], respectively. On the other hand, Blanco et al. [38] studied the solvent and substituent effects on the conformational equilibria and the strength of the intramolecular hydrogen bond of 4-substituted-2-hydroxybenzaldehydes by means of B3LYP/6-31G(d). These works did not address the spectral properties that we investigated here.

In the present study, the UV/Vis absorption spectra of 29 chalcone derivatives with a substituent on one or two phenyl rings are investigated by TD-DFT and polarizable continuum TD-DFT (PCM-TD-DFT) with the Perdew–Burke–Ernzerhof's (PBE1PBE) hybrid functional. The relationship between the absorption spectra and structure and the effect of substituents on electronic spectra are discussed.

2. Computational Details

We have chosen the GAUSSIAN03 [39] program to perform geometry optimizations, vibrational frequency determinations and excited state evaluations. From our previous investigation [35], it turned out that the oneparameter modified PBE1PBE hybrid functional [40] combined with Pople's split valence double-ζ singly polarized atomic basis set, 6-31G(d), provides adequate ground-state geometries which are in fairly good agreement with experimental data for chalcones. For instance, the deviations of the calculated bond lengths and angles of chalcone are less than 0.03 Å and 1°, respectively. Therefore, in this study the ground-state geometry of each molecule has been fully optimized at PBE1PBE/6-31G(d) level. In PBE1PBE, the percentage of exact, i.e., Hartree-Fock (HF), exchange amounts to 25%. For each geometry, vibrational frequencies were calculated analytically at the same level of theory as in the previous step, to ensure it to be a true local minimum.

After the ground-state geometry optimization, the excitation spectrum of each molecule has been

computed with TD-DFT at the PBE1PBE/6-31G level. This selection of basis set and functional is justified by a previous investigation [35] that clearly indicated that (a) the addition of polarization functions does not bring any significant improvement to the calculation of excitation energies; (b) adding extra polarization functions to 6-311G(d,p) increases the λ_{max} by only 1 nm, suggesting that the second set of polarization functions is unnecessary; (c) adding diffuse functions does not improve the calculated results; (d) pure-DFT functionals (such as BLYP) provide too small excitation energies with respect to experimental data, whereas the best accuracy is reached by using the 25% functionals, especially PBE1PBE. Since solvent effects play an important role in the absorption spectra of chalcones, in this paper, the polarizable continuum model (PCM) [41-43] dealing with solvent effect was chosen for the excitation energy calculations. In PCM, one divides the problem into a solute part (chalcones) lying inside a cavity, and a solvent part (in this work, ethanol) represented as a structureless material, characterized by its dielectric constant as well as other macroscopic parameters. Because we study UV/Vis spectra, we have selected the non-equilibrium PCM solutions.

3. Results and Discussion

3.1. Ground state geometries

The α,β -double bond is always considered to exist in the trans configuration, since the cis configuration is unstable due to the strong steric effects between the B-ring and the carbonyl group. According to previous calculation [35], the trans configuration is indeed more stable than the cis one. Thus, only the trans configuration was considered in this study. Table 1 lists the key geometric parameters of trans-chalcones obtained at the PBE1PBE/6-31G(d) level of calculation. According to our calculations, all the substituted molecules adopt the cis conformation, in agreement with an unsubstituted chalcone. From a comparison of the bond lengths and angles of substituted chalcones with that of unsubstituted one, it appears that the corresponding values are not very much different, the largest differences are less than 0.02 Å for bond lengths and 1° for bond angles. This indicates that introduction of a substituent has little effect on these geometric parameters. From torsion angle data (Table 1), it can be seen that the enone unit in each molecule is essentially planar, with an O10-C9-C8-C7 torsion angle of an average 3.9°, suggesting that an extended electron conjugated system is induced in the molecule. On the other hand, the phenyl A-rings are not coplanar with the enone system with an average 11.9° angle between the A-ring and the enone system (C6'-

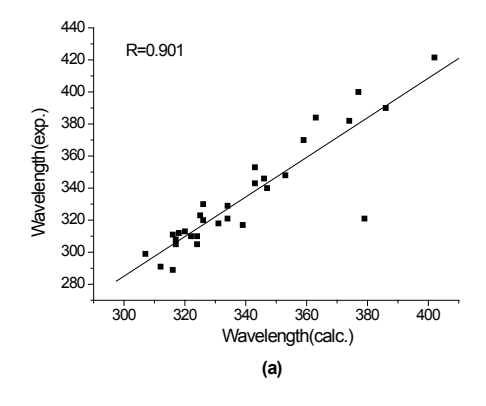
Table 1. Selected key structural parameters of chalcone and its derivatives from the PBE1PBE/6-31G(d) calculations.

Parameters	н	4'- Me	4- Me	4'- CI	4- CI	4'-Br	4- Br	4'-OMe	4- OMe	4'-OH	4- OH	4'-NH ₂	4- NH ₂	4'-NMe ₂	4- NMe ₂	4'-NO ₂	4- NO ₂
Bond lengths (Å)																	
R(1',9)	1.497	1.494	1.497	1.497	1.496	1.497	1.496	1.489	1.498	1.490	1.498	1.485	1.499	1.483	1.500	1.503	1.493
R(9,10)	1.225	1.225	1.225	1.225	1.225	1.225	1.225	1.226	1.226	1.226	1.226	1.227	1.227	1.228	1.227	1.224	1.224
R(8,9)	1.479	1.480	1.478	1.478	1.481	1.478	1.481	1.481	1.476	1.481	1.476	1.482	1.473	1.483	1.472	1.474	1.485
R(7,8)	1.345	1.345	1.345	1.346	1.345	1.346	1.345	1.345	1.347	1.345	1.347	1.344	1.349	1.344	1.350	1.347	1.344
R(1,7)	1.458	1.456	1.458	1.457	1.457	1.457	1.457	1.458	1.452	1.458	1.452	1.459	1.449	1.459	1.447	1.456	1.459
Bond angles (°)																	
A(2', 1',9)	117.4	117.3	117.6	117.3	117.2	117.2	117.3	117.4	117.3	117.6	117.3	117.7	117.3	117.7	117.3	117.2	117.2
A(1',9,10)	119.8	119.7	119.9	119.5	119.9	119.5	119.9	119.9	119.6	120.0	119.6	120.3	119.4	120.3	119.3	119.1	120.2
A(10,9,8)	121.2	121.2	121.0	121.3	120.9	121.3	120.9	120.7	121.3	120.8	121.3	120.6	121.5	120.4	121.6	121.9	120.5
A(9,8,7)	119.6	119.6	119.7	119.6	119.4	119.5	119.5	119.5	119.5	119.7	119.5	119.7	119.6	119.5	119.6	119.5	119.4
A(8,7,1)	128.0	128.1	128.0	128.0	128.0	128.1	127.9	128.1	128.3	127.9	128.3	127.9	128.5	128.1	128.5	128.1	127.6
A(7,1,2)	118.5	118.7	118.5	118.4	118.6	118.4	118.6	118.5	118.9	118.5	118.8	118.6	119.1	118.5	119.3	118.4	118.3
Torsion angles(°)																	
D(6', 1',9,8)	14.7	13.2	14.2	12.4	13.1	11.2	12.4	7.6	14.3	9.8	14.2	8.2	-14.7	0.2	14.2	17.1	11.8
D(8,7,1,6)	1.7	2.7	0.8	2.1	0.6	0.5	0.4	0.7	0.0	2.8	0.5	3.1	-0.2	0.0	0.0	2.0	0.6
D(10,9,8,7)	5.0	5.2	4.2	4.9	4.1	3.9	4.1	3.2	3.8	4.6	4.0	4.0	-3.7	0.1	3.7	5.1	4.2
D(2', 1',9,10)	12.7	11.1	12.2	10.5	11.3	9.5	10.6	6.4	12.3	8.1	12.3	6.7	-12.7	0.1	12.3	14.8	10.1

C1'-C9-C8), while phenyl B-rings are almost coplanar with the enone system with an average 1.1° angle between them (C8-C7-C1-C6). By comparison, we find that the corresponding torsion angles of substituted chalcones are also not very much different from the unsubstituted one, which indicates that substitution does not substantially distort the molecular skeleton. It is interesting to note that molecule 4'-NMe₂ has an unexpected fully planar structure with an average torsion angle of only about 0.1°.

3.2. Electronic spectra

The calculated absorption characteristics together with experimental values for chalcone derivatives in ethanol are summarized in Table 2. It can be seen from Table 2 that the lowest lying singlet excited states for all the title compounds comprise an electronic transition primarily between the highest occupied molecular orbital (HOMO) and the lowest unoccupied molecular orbital (LUMO). Molecular orbital coefficients analysis (not shown) indicates that the frontier molecular orbitals are mainly composed of p atomic orbitals, so the lowest lying singlet—singlet absorptions correspond to $\pi{\to}\pi^*$ type electronic transitions. To further explore the performance of the procedure, we first compared our calculated results with experimental values. A graphical comparison can be found in Fig. 2. We note that there



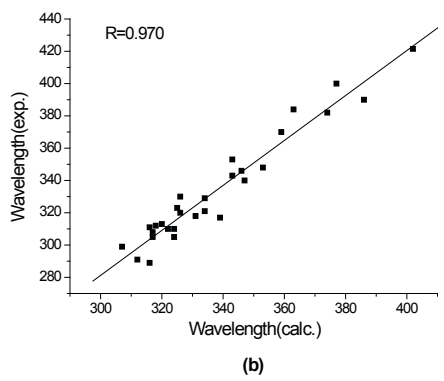


Figure 2. The relationship between experimental and theoretical λ_{max} for chalcones with (a) and without (b) 8a.

are some discrepancies between the experimental values reported in the literature. This illustrates that experimental values are never completely error-free. In cases for which multiple measurements do exist, the average value has been taken as experimental data.

As can be seen from Table 2, the agreement between theoretical and experimental values is excellent, especially for halogens and alkyl substituents, whereas sizable differences appear for nitro substituents, especially when presents on phenyl ring A. A statistical analysis of the data in Table 2 gives a mean absolute error of 0.136 eV

or 12 nm, which is smaller than the usual expected accuracy of TD-DFT (0.2–0.3 eV). Except for molecule 8a, the maximal absolute deviation is limited to 0.37 eV (27 nm), with only 4 cases for which the errors exceed 0.20 eV (20 nm). Consistently, the correlation coefficient (R) obtained by simple linear regression (Fig. 2) is larger than 0.9 in both the wavelength and energetic scales. It can be seen from Fig. 2a that only the strong electron withdrawing substituent (4'-NO $_2$) deviats from the fitted line, the deletion of this substituent improves the correlation significantly (Fig. 2b).

Table 2. Calculated and observed substituent effects on the λ_{max} (in nm) and molecular orbital energies (in eV) of chalcones.

			λ max			Assignment		shift				
Comp.	Substitution	E(eV)	calc. exp. b		f	(CI coeff.)	calc. exp. b		номо	LUMO	H-L	
CH	Н	3.9273	316	309,313°	0.9012	H→L (82%)	0	0	-6.60	-2.00	4.60	
1a	4'-Me	3.9106	317	308	0.9961	H→L (81%)	1	-1	-6.55	-1.93	4.62	
1b	4-Me	3.8090	326	330	0.9592	H→L (83%)	10	21	-6.41	-1.92	4.48	
2a	4'-CI	3.8485	322	310	0.9491	H→L (82%)	6	1	-6.71	-2.17	4.54	
2b	4-Cl	3.8700	320	312	1.0133	H→L (83%)	4	3	-6.66	-2.17	4.49	
3a	4'-Br	3.8314	324	305	0.9896	H→L (82%)	8	-4	-6.71	-2.17	4.53	
3b	4-Br	3.8255	324	310	1.0263	H→L (84%)	8	1	-6.62	-2.18	4.44	
4a	4'-OMe	3.7986	326	320	0.9938	H→L (89%)	10	11	-6.38	-1.84	4.54	
4b	4-OMe	3.6109	343	341-345	0.9527	H→L (82%)	27	32-36	-6.07	-1.80	4.27	
5a	4'-OH	3.8177	325	321	0.9616	H→L (89%)	9	12	-6.46	-1.87	4.59	
5b	4-OH	3.6164	343	351-355	0.8763	H→L (79%)	27	42-46	-6.14	-1.83	4.31	
6a	4'-NH ₂	3.4525	359	370	0.6894	H→L (87%)	43	61	-5.94	-1.71	4.23	
6b	4-NH ₂	3.2865	377	400	0.9235	H→L (84%)	61	91	-5.70	-1.67	4.03	
7a	4'-NMe ₂	3.2112	386	393,387°	0.7023	H→L (89%)	70	84,74°	-5.56	-1.63	3.93	
7b	4-NMe ₂	3.0854	402	425,418°	0.9680	H→L (85%)	86	116,105°	-5.41	-1.59	3.81	
8a	4'-NO ₂	3.2712	379	325	0.2119	H→L (71%)	63	16	-6.92	-2.77	4.15	
8b	4-NO ₂	3.6539	339	317	0.9742	H→L (82%)	23	8	-7.26	-2.87	4.39	
9	2,4-diCl	3.9239	316	289	0.9748	H→L (82%)	0	-23				
10	3,4-diCl	3.9118	317	305	1.0231	H→L (82%)	1	-7				
11	2-Cl	3.9788	312	295	0.7956	H→L (81%)	-4	-14				
12	4'-Cyclohexyl	3.8921	318	312	1.0528	H→L (81%)	2	0				
13	3-CF ₃	4.0403	307	299	0.9345	H→L (79%)	-9	-13				
14	4', 4-diOMe	3.5765	347	340 ^d	0.9643	H→L (77%)	31	28 ^d				
15	4'-EtO, 4-OMe	3.5886	346	346°	0.9756	H→L (72%)	30	34 ⁰				
16	4'-Br, 4-OMe	3.5152	353	348e	0.7288	H→L (64%)	37	35.5 ⁰				
17	4'-OMe, 4-Br	3.7170	334	321 ⁰	1.0923	H→L (90%)	18	9 e				
18	2',4',6'-triMe, 4-OMe	3.7082	334	329 °	1.0075	H→L (77%)	18	17 e				
19	4'-OMe, 2,4,6-triMe	3.7482	331	318 ⁰	0.7782	H→L (63%)	15	6 ^e				
20	3',4'-diOH, 3,4-diOH	3.4201	363	384 ^f	0.7042	H→L (85%)	47	72 ^f				
21	2',4'-diOH, 3,4-diOH	3.3138	374	382 ^g	0.8095	H→L (86%)	58	72.5 ⁹				

all experimental results in ethanol; [44]; [45]; [46]; [48]; [48]; [48], the shift is calculated on the basis of a 309.5 nm value for the parent compound.

The observed substituent effects are reproduced by calculation qualitatively. For instance, the ratio of the calculated shift for 4a and 4b (~1:3) is in good agreement with the experimental value. This is also the case for other chalcones. Interestingly, although the absolute deviation of λ_{max} for 8a is slightly too large (58 nm), the substituent effect is reproduced well by calculation. The ratio of the calculated shift for 8a and 8b (2.7:1) is in good agreement with the experimental value (2:1).

In our set of compounds, the largest discrepancy between theory and experiment shows up for 4'-NO, substitution (8a). For the strongly polar NO, group it is often difficult to model precisely with conventional DFT approaches. We predict large shifts of 63 and 23 nm from unsubstituted chalcone for 4'-NO2 and 4-NO2, respectively, whereas the experimental results give smaller shifts of 16 and 8 nm, which are 3~4 times smaller than the former. This could be the consequence of specific interactions, such as hydrogen bonds formed between solvent (ethanol) and solute (chalcones), but PCM is unable to take them into account. We notice that such short-sightedness of the PCM model has also been observed previously [50,51]. On the other hand, as will be shown later, charge transfer valenceexcited states might occur in molecule 8a. It is well known that such states are not well described by TD-DFT within the generalized adiabatic approximation and with the usual exchange-correlation functionals [30, 52-54]. This may be another reason for the large discrepancy (~58 nm) between the theoretical and experimental λ_{max} for 8a.

3.3. The effect of substitution on absorption spectra

First we consider the monosubstituted species. As can be seen from Table 2, the λ_{max} of substituted chalcones presents bathochromic effects when the hydrogen atom at the para-position in the phenyl ring is replaced by a substituent. By comparison, we find that the bathochromic effects of strongly positive electromeric substituents such as NMe2, NH2, OH and OMe are 1.2-3.0 times greater when the groups are located on phenyl ring B than on ring A. Weakly positive groups such as Me, Cl and Br have small bathochromic effects when present on ring B and are practically no consequence when present on ring A. Thus, the λ_{max} of the substituted chalcone on phenyl ring A is less sensitive to substitution than that on ring B. This coincides with the conclusion drawn in a previous study [35] that the intense excitation corresponding to this peak is mainly localized on the phenyl ring B. Contrary to other substituents, the bathochromic effect is about 2 times greater when the group is located on phenyl ring A than on ring B for a strong electron withdrawing group such as NO₂. This also may be due to the significant charge transfer occuring in molecule 8a as mentioned above.

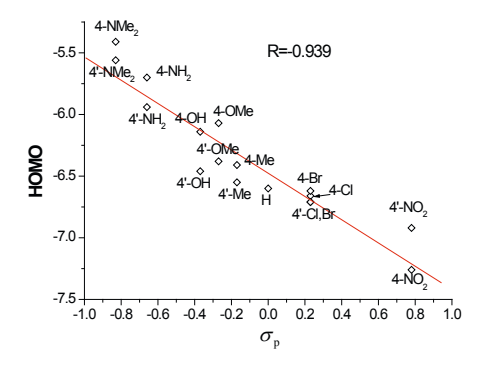
From Table 2, it can also be found that the sequence of the λ_{max} is 1a < 2a \approx 3a <4a \approx 5a <6a<7a and 2b<3b<1b<4b=5b<6b<7b for substitution on phenyl ring A and B, respectively. These orderings are nearly identical to corresponding experimental results: 3a<1a≈2a<4a<5a<6a<7aand2b≈3b<1b<4b<5b<6b<7b, respectively. The effect of substitution on absorption spectra can be explained as following: for the electron donating substituents in para-positions, the lone electron pair of nitrogen or oxygen of NMe, NH, OH, OMe, and C-H σ-bond of Me join in molecular conjugation, which makes the conjugated-system of molecules become larger. In addition, the electron donating ability of substituents is ordered as NMe₂ > NH₂ > OH > OMe > Me, and the order of λ_{max} is 7 > 6 >5 > 4 > 1. The substituents CI and Br result in minor changes to λ_{max} relative to that of unsubstituted chalcones, which is indicative of the induced electron attraction, as well as the joining of unshared electron pairs of chlorine and bromine in the conjugation for molecule 2 and 3.

In the case of di-substituted compounds with both substituents of strongly positive electromeric character, the resulting bathochromic effects are of the same magnitude as those caused by only one group present on ring B (compare 14-4b, 15-4b). On the other hand, the bathochromic effect caused by a strong positive electromeric group is retained in the presence of weakly positive groups (compare 17-4a, 19-4a).

It has been observed that the substitutions of electron donating and withdrawing groups slightly increase the oscillator strength values compared to neutral chalcones, with an exception of a few cases (e.g. 6a, 7a or 8a). The largest decrease is observed in the substitution of NO₂ at phenyl ring A (8a) with an unusually low oscillator strength (f=0.2119). This is likely due to the vanishing overlap between the MOs involved in the corresponding electronic transition (see Fig. 4), which usually results in a very low oscillator strength [30].

3.4. Frontier orbital analysis

It is useful to examine the HOMOs and the LUMOs for molecules to provide the framework for the excited state. Furthermore, the relative ordering of the occupied and virtual orbitals provides a reasonable qualitative indication of the excitation properties [55]. The last three columns of Table 2 summarize the comparison of the energy levels of the HOMO, LUMO, and their gap (HOMO–LUMO) for chalcones. In order to illustrate the effect of substituents on the HOMO and LUMO energies, the values of their energies were plotted against Hammett's substituent constants $(\sigma_{\rm p})$ [56] (as shown in Fig. 3). It can be seen from Fig. 3 that the $\sigma_{\rm p}$ correlates linearly with HOMO and LUMO energies with



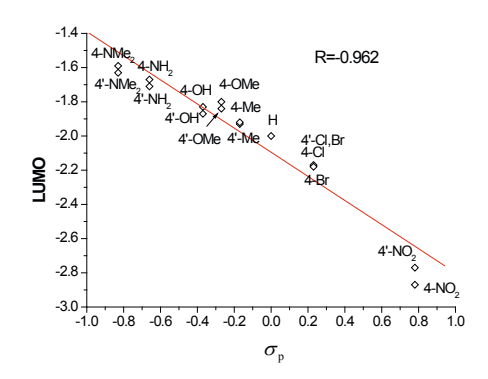


Figure 3. The relationship between the energies of HOMO (left) and LUMO (right) and Hammett constants σ_p

negative slope, in other words, the substituent effect on HOMO and LUMO is straightforward: the electron donating groups (e.g. Me, OH, NH2, NMe2 or OMe) cause increasing (become more positive) orbital energy, while the electron withdrawing groups (e.g. Cl, Br or NO₂) cause decreasing orbital energy. The correlation coefficients of $\sigma_{\rm p}$ with LUMO and HOMO energies are 0.962 and 0.939 respectively. It has been observed from Table 2 that the HOMO-LUMO gap of unsubstituted chalcone is higher than those of the substituted one. For instance, the substitution of NMe, decreases the HOMO-LUMO energy gap greatly, which possesses the lowest absorption energy and the highest absorption wavelength compared to other substitutents. This implies that it is easier to promote an electron from the HOMO to the LUMO by substituting the relevant electron donating and withdrawing groups, and will results in a red shift of the absorption spectrum.

To gain further insight into the nature of the electronic transition, the electron density plots of the HOMO and LUMO for monosubstituted chalcones are presented in Fig. 4, along with those of unsubstituted one for comparison. From Fig. 4, it can be seen that the plots of the HOMO and LUMO of chalcones demonstrate the typical $\pi\text{-type}$ molecular orbital characteristics. The introduction of electron donating and withdrawing groups alters the nature of delocalization and consequently determins the electronic properties of the molecules. It was observed that the substitution in phenyl ring A alters the nature of the delocalization greatly compared to the substitution in ring B.

First we describe the 4-substituted species. The pattern of the HOMOs and LUMOs are qualitatively similar with each other, except for the NO₂ group. As can be seen from Fig. 4, strong delocalization is present in the LUMOs, whereas the HOMOs show more localization of the isosurfaces of the wave functions on the cinnamoyl moiety. Thus, these states correspond to

an electron transfer from cinnamoyl moiety to the whole molecular skeleton. A comparison with unsubstituted chalcones shows that the main contributions of HOMO and LUMO do not change significantly, and are still centred on the cinnamoyl moiety and the molecular skeleton, respectively, and will further spread to the conjugated substituent. Clearly, the introduction of substituents in para positions of phenyl ring B elongates the conjugated system and leads to a decrease of the excitation energy (red shift of the $\lambda_{\rm max}$). In contrast to other species, the 4-NO₂ substituted chalcone (8b) exhibits different transition characteristic. The HOMO is delocalized over the entire backbone of the molecule; however, the LUMO is localized on the cinnamoyl moiety and nitro group.

Turning now to the 4'-substituted chalcones. It was found that the main contributions of LUMOs do not change significantly compared to that of 4-substituted chalcones, while those of HOMOs differ depending on the nature of the substituent. Similar to the unsubstituted chalcone, for 4'-Me, 4'-Cl and 4'-Br, the HOMOs and LUMOs are still centred on the cinnamoyl moiety and the molecular skeleton, respectively. Note that the substituted groups almost do not play any role in the MOs. Thus, the shifts of λ_{max} from unsubstituted chalcones for these compounds are small, with a calculated average shift of only 5 nm. As for 4'-OMe and 4'-OH, both the HOMOs and LUMOs are mainly delocalized over the molecular skeleton as well as the oxygen atom of the substituent. Note that the electron density on the carbonyl group is equal to zero, indicating that the carbonyl group does not play any role in the HOMO. By comparison, similar characteristics of electron density distributions are found between 4'-NH, and 4'-NMe₂. In contrast to 4-NH₂ the 4-NMe₂, HOMOs are localized on the benzoyl moiety with substantial contributions from their respective substituents, whereas LUMOs are distributed on the molecular skeleton with a small contribution from the substituent. For 4'-NO,

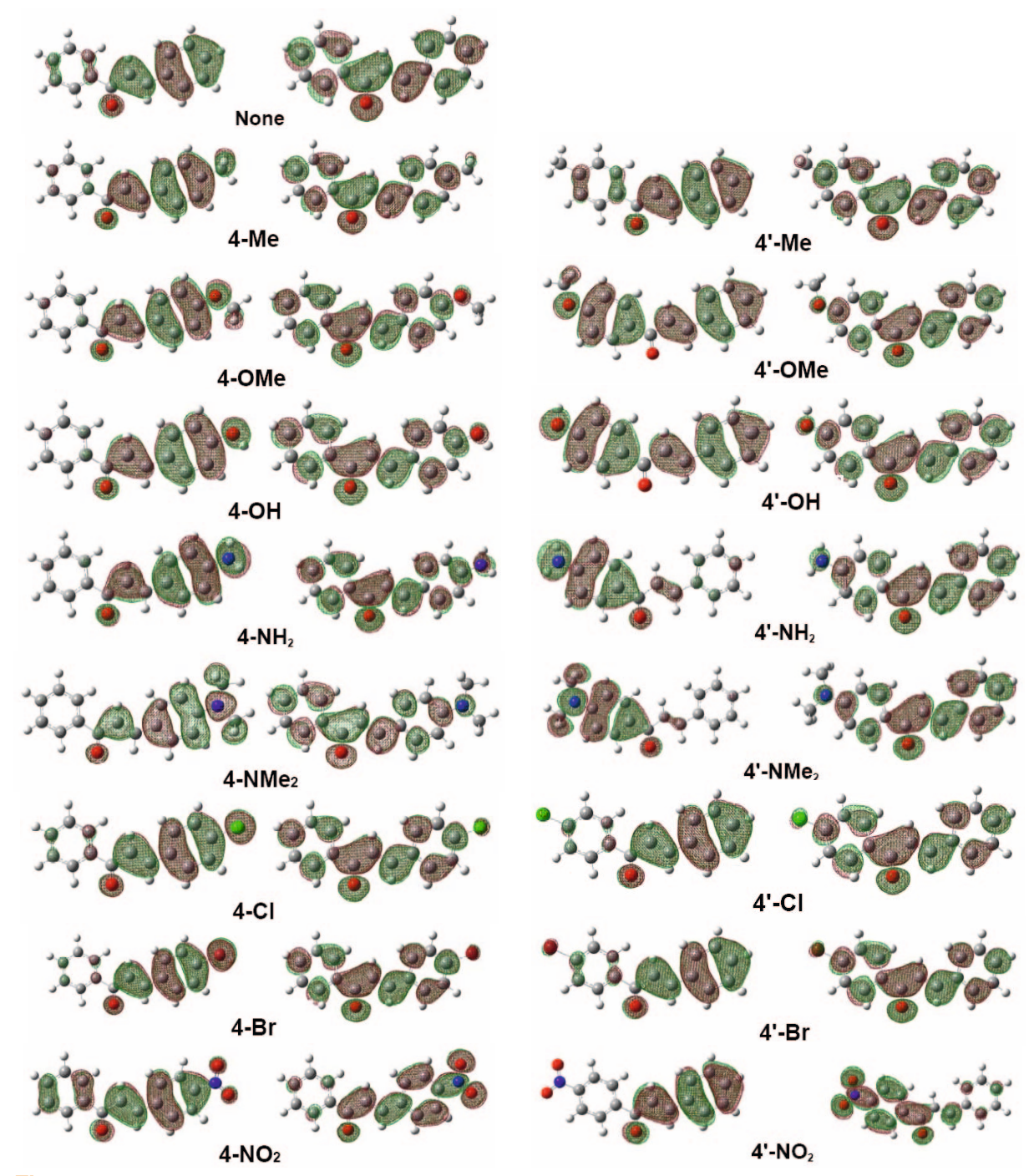


Figure 4. The electron density plots of the HOMO(from left to right, the first and third column of panels) and LUMO(from left to right, the second and fourth column of panels) of para-monosubstituted chalcones.

(8a), the HOMO resides wholly at the cinnamoyl moiety, whereas the LUMO is localized at the benzoyl fragment as well as the nitro group.

It is noteworthy that except for 8a, all other HOMOs show substantial overlapping with the corresponding delocalized LUMOs. This suggests that most transitions should be of a valence excitation nature, though

transitions from the somewhat localized HOMOs are expected to have partial charge transfer character. On the other hand, a transition from HOMO to LUMO in 8a should be of charge-transfer character due to near-zero orbital overlap (Fig. 4), occurring primarily at the oxygen and carbon atom in the enone moiety. As mentioned above, the system with significant charge transfer

character is known to be a difficult case for DFT, which tends to overshoot the amount of transferred charge and consequently underestimates the excitation energy. Of course, selecting a range-separated hybrid, like the Coulomb-attenuated model (CAM-B3LYP), or using conventional hybrids including at least 50% of exact exchange could correct the TD-DFT value, but at the price of a likely loss of accuracy for the transitions with a more localized character [57]. It is notable that for 4-NO₂ (8b), one has a significant overlap between the HOMO and LUMO orbitals on one of the two aromatic rings. This explains how TD-PBE1PBE does lead to satisfactory results for this molecule.

4. Conclusions

We have investigated the structures and spectral properties of substituted chalcones using DFT and TD-DFT. Comparisons with experimental values lead to a mean absolute error of 12 nm (0.136 eV). Moreover, the observed substituent effects are reproduced by calculation qualitatively, confirming the reliability of the PCM-PBE1PBE/6-31G // PBE1PBE/6-31G(d) level of theory to investigate the ground and excited state properties. The $\lambda_{\rm max}$ of substituted chalcones on phenyl ring A is less sensitive to substitution than that on ring B.

References

- [1] S. Murakami, M. Muramatsu, H.Aihara, Biochem. Pharmacol. 42, 1447 (1991)
- [2] R.J. Anto, et al., Cancer Lett. 97,33 (1995)
- [3] N.J. Lawrence, A.T. McGown, Curr. Pharm. Design, 11, 1679 (2005)
- [4] Z. Nowakowska, Eur. J. Med. Chem. 42,125 (2007)
- [5] M. Liu, P. Wilairat, M.L. Go, J. Med. Chem. 44,4443 (2001)
- [6] D. Batovska, Eur. J. Med. Chem. 42, 87 (2007)
- [7] J.H. Wu, X.H. Wang, Y.H. Yi, Bioorg. Med. Chem. Lett. 13,1813 (2003)
- [8] L. Mathiesen, K.E. Malterud, R.B. Sund, Planta Med. 61,515 (1995)
- [9] M.P. Cockerham, C.C. Frazier, S. Guha, E.A. Chauchard, Appl. Phys. B53,275 (1991).
- [10] B.K. Sarojinia, B. Narayanab, B.V. Ashalathab, J. Indirac, K.G. Lobo, J. Cryst. Growth 295, 54 (2006)
- [11] H.J. Ravindra, K. Chandrashekaran, W.T.A. Harrison, S.M. Dharmaprakash, Appl. Phys. B94, 503 (2009)
- [12] P. Poornesh, et al., Opt. Mater. 31, 854 (2009)
- [13] S. Shettigar, K. Chandrasekharan, G. Umesh, B.K. Sarojini, B. Narayana, Polymer 47, 3565 (2006)

The sequences of the calculated λ_{max} are nearly identical to the corresponding experimental results. The HOMO and LUMO energies and their energy gaps are shifted due to the substitution of electron donating and electron withdrawing groups, and the linear correlation of Hammett's substituent constants (σ_n) with LUMO energies is better than with HOMO energies, and the correlation coefficients are 0.962 and 0.939, respectively. The calculation reveals that the maximum absorption band mainly results from the $\pi \rightarrow \pi^*$ transition from the HOMO to the LUMO. Moreover, most transitions should be of a valence excitation nature. The calculation results also give good evidence of the intramolecular charge transfer nature of the HOMO

LUMO transitions for the 4'-NO, molecule (8a).

Acknowledgements

This work was supported by the Natural Science Foundation of Jiangsu Province (Grant No. BK2009523) and the Science Research Startup Foundation of Xuzhou Medical College (No.07KJ51).

Supplementary material available

The Cartesian coordinates of the optimized structures in gas at PBE1PBE/6-31G(d) level for chalcones.

- [14] P.S. Patila, et al., J. Cryst. Growth 303, 520 (2007)
- [15] P.S. Patila, S.M. Dharmaprakasha, H.K. Funb, M.S. Karthikeyan, J. Cryst. Growth 297, 111 (2006)
- [16] A.A. Sukhorukov, B.A. Zadorozhnyi, V.F. Lavrushin, Theor. Exp. Chem.6,490 (1973)
- [17] M. Reinkhardt, A.A. Sukhorukov, A. Raushal, V.F. Lavrushin, Chem. Heterocyclic. Comp.13,969 (1977)
- [18] V.G. Mitina, A.O. Doroshenko, A.A. Sukhorukov, V.F. Lavrushin, Theor. Exp. Chem.20,141(1984)
- [19] V.L. Gineitite, G.A. Gasperavichene, Theor. Exp. Chem.25,247(1989)
- [20] K. Ohno, Y. Itoh, T. Harnada, M. Isogai, A. Kakuta, Mol. Cryst. Liq. Cryst. A182, 17 (1990)
- [21] K. Gustav, R. Colditz, A. Jabs, J. Prakt. Chem. 332, 645 (1990)
- [22] M. Oumi, D. Maurice, M.H.Gordon, Spectrochim. Acta A55, 525 (1999)
- [23] K.S. David, et al., J. Am. Chem. Soc. 128, 12243 (2006)
- [24] I. Ciofini, P.P. Lainé, F. Bedioui, C. Adamo, J. Am. Chem. Soc. 126, 10763 (2004)
- [25] D. Jacquemin, et al., J. Chem. Phys. 121, 1736 (2004)

- [26] D. Jacquemin, J. Preat, V. Wathelet, M. Fontaine, E.A. Perpete, J. Am. Chem. Soc.128, 2072 (2006)
- [27] B.B. Koleva, T. Kolev, R. Nikolova, Y. Zagraniarsky, M. Spiteller, Cent. Eur. J. Chem. 6, 592 (2008)
- [28] D. Jacquemin, E.A. Perpte, I. Ciofini, C. Adamo, Acc. Chem. Res. 42, 326 (2009)
- [29] N. Santhanamoorthi, K. Senthilkumar, P. Kolandaivel, Mol. Phys. 107, 1629 (2009)
- [30] Z.W. Qu, H. Zhu, V. May, J. Phys. Chem. B113, 4817 (2009)
- [31] S. Lunak Jr. et al., Dyes Pigments 85, 27 (2010)
- [32] I.F.Janczareka et al., Spectrochim. Acta A72, 394 (2009)
- [33] A. Amat, C. Clementi, F. De Angelis, A. Sgamellotti, S. Fantacci, J. Phys. Chem. A113, 15118 (2009)
- [34] L.Serrano-Andres, M. Merchan, J. Mol. Struct. (Theochem.) 729, 99 (2005)
- [35] Y.S. Xue, X.D. Gong, J. Mol. Struct. (Theochem.) 901, 226 (2009)
- [36] L.D. Hicks, A.J. Fry, V.C. Kurzweil, Electrochim. Acta. 50, 1039 (2004)
- [37] D. Kozlowski et al., J. Phys. Chem. A, 111, 1138 (2007)
- [38] S.E. Blanco, F.H. Ferretti, Tetrahedron Lett. 48, 2577 (2007)
- [39] M. J. Frisch et al. Gaussian 03, Revision B.03 (Gaussian, Inc., Pittsburgh PA, 2003)
- [40] J.P. Perdew, K. Burke, M. Ernzerhof, Phys. Rev. Lett. 78, 1396 (1997)
- [41] C. Amovilli *et al.*, Adv. Quantum Chem. 32, 227 (1998)

- [42] M. Cossi, V. Barone, J. Chem. Phys. 115, 4708 (2001)
- [43] C. Adamo, V. Barone, Chem. Phys. Lett. 330, 152 (2000)
- [44] H.H. Szmant, A.J. Basso, J. Am. Chem. Soc. 74, 4397 (1952)
- [45] E.R. Katzenellenbogen, G.E.K. Branch, J. Am. Chem. Soc. 69, 1615 (1947)
- [46] P.W. Shen, C. Zheng, D. Zhang, Y.X. Che, J. Synth. Cryst. 21, 280 (1992)
- [47] I.F. Verpuson, R.P. Barnes, J. Am. Chem. Soc. 70, 3907 (1948)
- [48] A. Russel, J. Todd, C.L. Wilson, J. Chem. Soc. 1940 (1934)
- [49] M.K. Seikel, T.A. Geissman J. Am. Chem. Soc. 72, 5720 (1950)
- [50] D. Jacquemin, J. Preat, V. Wathelet, E.A. Perpète, J.Chem.Phys. 124, 074104 (2006)
- [51] D. Jacquemin, E.A. Perpète, Theor. Chem. Account 120, 405 (2008).
- [52] D.J. Tozer, R.D. Amos, N.C. Handy, B.O. Roos, L. Serrano-Andres, Mol. Phys. 97, 859 (1999)
- [53] A. Dreuw, M.H. Gordon, J. Am. Chem. Soc. 126, 4007 (2004)
- [54] A. Dreuw, M.H. Gordon, Chem. Rev. 105, 4009 (2005)
- [55] M.A. De Oliveira, H.A. Duarte, J.M. Pernaut, W.B. De Almeida, J. Phys. Chem. A104, 8256 (2000)
- [56] C. Hansch, A. Leo, R.W. Taft, Chem. Rev. 91, 165 (1991)
- [57] D. Jacquemin, E.A. Perpète, G.E. Scuseria, I. Ciofini, C. Adamo, J. Chem. Theory Comput. 4, 123 (2008)